



Nonreactive deposition of Ti_3SiC_2 thin film by sputtering elemental targets using a magnetized sheet plasma source

Hamdi Muhyuddin Barra^{1*}, *Henry Ramos*²

¹*Department of Physics, Mindanao State University-Main Campus, Marawi City, 9700, Philippines.*

²*National Institute of Physics, University of the Philippines – Diliman, Quezon City, 1101, Philippines.*

Abstract

This study presents the synthesis of the MAX phase compound Ti_3SiC_2 by sputtering titanium, silicon, and graphite targets using a magnetized sheet plasma source. Ti_3SiC_2 thin film on stainless steel and polycarbonate substrates was prepared with different deposition time of 60, 90, and 120-min. X-ray diffraction (XRD) scans of the samples showed the effective synthesis of Ti_3SiC_2 as the stoichiometric peaks corresponding to the (002), (104), (116), and (1013) facets of Ti_3SiC_2 were detected. Further, scanning electron micrograph (SEM) images of the samples revealed that increasing the deposition time resulted in a smoother surface and the formation of grain-like structures.

Keywords: MAX phase, Sheet plasma, Sputtering system, Titanium silicon carbide, Thin films

Full length article *Corresponding Author, e-mail: hamdimuhyuddin.barra@msumain.edu.ph

1. Introduction

Since its successful synthesis, MAX phase has become one of the prevalent thin film compounds that is synthesized and deposited on different materials [1-3]. This group of ternary compounds, with a formula $\text{M}_{n+1}\text{AX}_n$ ($n = 1, 2, \text{ or } 3$), is composed of an early transition metal, an A-group element, and C or N (the X factor). This layered carbide or nitride has caught the attention of researchers for its functional and industrial applications. This is primarily due to its useful properties as it combines the characteristics of metals and ceramics. For instance, it is electrically and thermally conductive, shock resistant, and damage tolerant at high temperature like metals, as well as oxidation and corrosion resistant, thermally stable, and has low density and high melting point like ceramics [4-9]. As such, MAX phase materials have great potential as heating elements, high-temperature bearings, electrocatalysts, photocatalysts, and nuclear fuel claddings [10-14]. Titanium silicon carbide (Ti_3SiC_2) is one of the most studied MAX phase materials. This nanolaminate compound has a layered hexagonal structure with excellent physical, electrical, and thermal properties. For instance, it has low density (4.52 g/cm^3), high fracture toughness ($7 \text{ MPa m}^{1/2}$), high elastic modulus (322 GPa), high melting point ($3200 \text{ }^\circ\text{C}$), good electrical conductivity ($4.5 \times 10^6 \text{ S/m}$) and remarkable thermal conductivity (34 W/mK) [15-18]. Ti_3SiC_2 is usually synthesized via physical vapor deposition using sputtering techniques [2]. Typically, Ti_3SiC_2 is synthesized via reactive sputtering using methane (CH_4) as the reactive gas.

Also, most of the methods employed require high deposition temperature. This limits the use of materials that have low melting points and are sensitive to high temperatures. Thus, there is an interesting need to find a method that lowers deposition temperature or one that does not require substrate heating. Consequently, the applications of the MAX phase in coating and surface modification industries would create opportunities for the use of temperature-sensitive substrates. Hence, in this work, the synthesis of Ti_3SiC_2 without applying substrate heating and biasing is presented. This novel route was achieved using a magnetized sheet plasma source. The thin film was deposited onto stainless steel substrate by sputtering titanium, silicon, and graphite targets with accelerated Ar plasma. To show that no substrate heating was employed, the deposition was also done onto a temperature-sensitive polycarbonate (PC) film.

2. Materials and methods

The sheet plasma negative ion source (SPNIS) facility with a magnetron configuration was utilized in the experimental runs. **Fig. 1** shows the schematic diagram of the magnetized sheet plasma source. Titanium, silicon, and graphite disks were used as sources of Ti, Si, and C, respectively. The targets were negatively biased with a potential of -1 kV and sputtered with Ar plasma generated in sheet form and accelerated at a discharge current of 4 A and discharge potential of 70 V .

Stainless steel type 316 substrates with dimensions of $15 \times 15 \times 0.5 \text{ mm}^3$ were placed 4 cm away from the targets and prepared with differing deposition time of 60, 90 and 120 min. These processing times were selected based on previous works conducted in the SPNIS device [19-20]. Accordingly, a 60-min deposition process resulted in high sputtering yield and deposition rate. Meanwhile, a processing time greater than 120 min may lead to re-sputtering of the deposited film. Moreover, the substrates were neither heated nor biased. The deposition was done at a gas-filling pressure of 6.0×10^{-3} Torr. The experimental setup used in the sputtering process is displayed in **Fig. 2**. The same parameters were used for a temperature-sensitive polycarbonate (PC) film with dimensions of $15 \times 15 \times 3 \text{ mm}^3$, albeit its distance to the sheet plasma was set at 3 cm. The samples were then characterized using X-ray diffraction (XRD) for crystal structure analysis and the confirmation of Ti_3SiC_2 synthesis. Further, scanning electron microscopy with an attached energy dispersive X-ray (EDX) spectroscopy (SEM, JEOL JSM 5310) was utilized to analyze the surface morphology of the samples and to validate the presence of the three elements of the desired MAX phase.

3. Results and Discussions

After the deposition process, the steel samples display metallic gray to blue-colored deposits while the PC samples exhibit brownish shades. Successful synthesis is validated by the EDX scan of the steel sample as shown in **Fig. 3**, which shows the presence of the three elements of the desired MAX phase. It must be noted that the unlabeled peaks are inherent in the stain-less steel type 316. Further, the superimposed XRD scans of the steel substrates in **Fig. 4** show the comparison of the coated and untreated samples. Accordingly, the graph exhibits the peaks at 2θ values of 9.60° , 38.5° , and 78.3° , which correspond to the (002), (104), and (1013) facets of Ti_3SiC_2 , respectively, as indexed in JCPDS No. 40-1132 [18].

It can also be observed that the sample prepared at 60-min deposition time did not display the (002) phase of Ti_3SiC_2 , but it exhibits the (116) phase of Ti_3SiC_2 at the 2θ value of 69.6° . Further, using the peak of the samples with the highest intensity ($2\theta \approx 78.3^\circ$), Table 1 summarizes the full width at half maximum (FWHM), peak intensity, crystallite size (D), and lattice strain (ϵ) of the samples. As seen, the intensities of the peak and the FWHM of the samples decreased when the deposition time was increased to 120 min. Correspondingly, there is an increase in the crystallite size and a decrease in the lattice strain when the deposition time was increased from 60 to 120 min. Indeed, this result indicates an increase in the crystallinity of the sample. In addition, the microstructures of the steel samples are shown in **Fig. 5** as observed through an SEM. It can be seen that the surface of the substrate with greater deposition time is smoother. Also, grain-like structures are formed as the deposition time was increased, which indicates the high plasticity of Ti_3SiC_2 . Meanwhile, **Fig. 6** displays the diffractograms of the Ti_3SiC_2 thin film deposited on polycarbonate substrates. As seen, the samples exhibit similar peaks to the steel substrates (**Fig. 3**). Likewise, the presence of the impurity, in the form of TiSi, is observed. Interestingly, the peak at 2θ value of 9.60° has substantially increased as the deposition time was increased from 60 to 120 min. Similar with the steel samples, the FWHM of the Ti_3SiC_2 thin-film deposited PC substrates decreased from 0.118 to 0.120 when the deposition time was increased from 60 to 120 min. As such, this indicates an increase in the crystallinity of the sample. Indeed, these findings reveal that synthesis of Ti_3SiC_2 using the SPNIS can be carried out without applying bias and heating to a substrate. Finally, the scanning electron microscopy scans in **Fig. 7** show that the samples became smoother as the deposition time was increased. Like the steel substrates, prolonging the duration of deposition resulted in the reduction of the impurities in the samples.

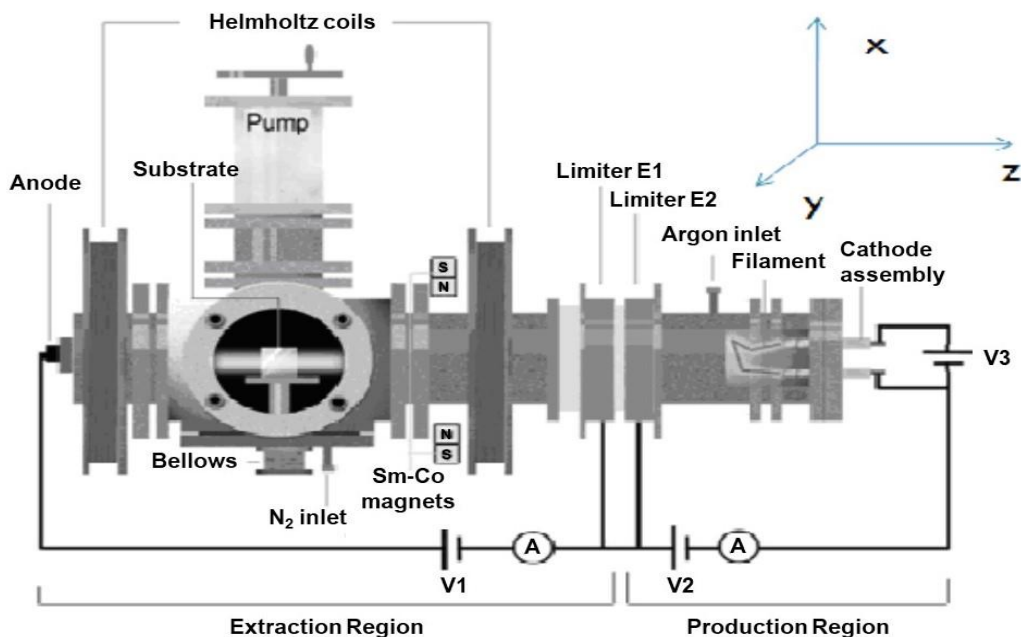


Fig. 1. Schematic diagram of the SPNIS [19].

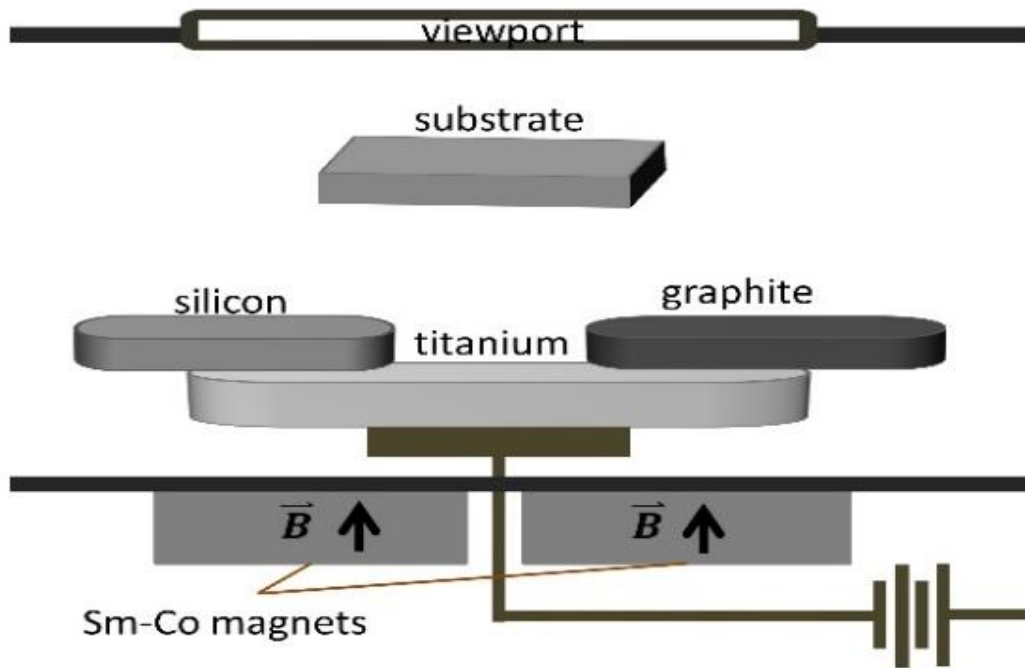


Fig. 2. Experimental setup of the sputtering process.

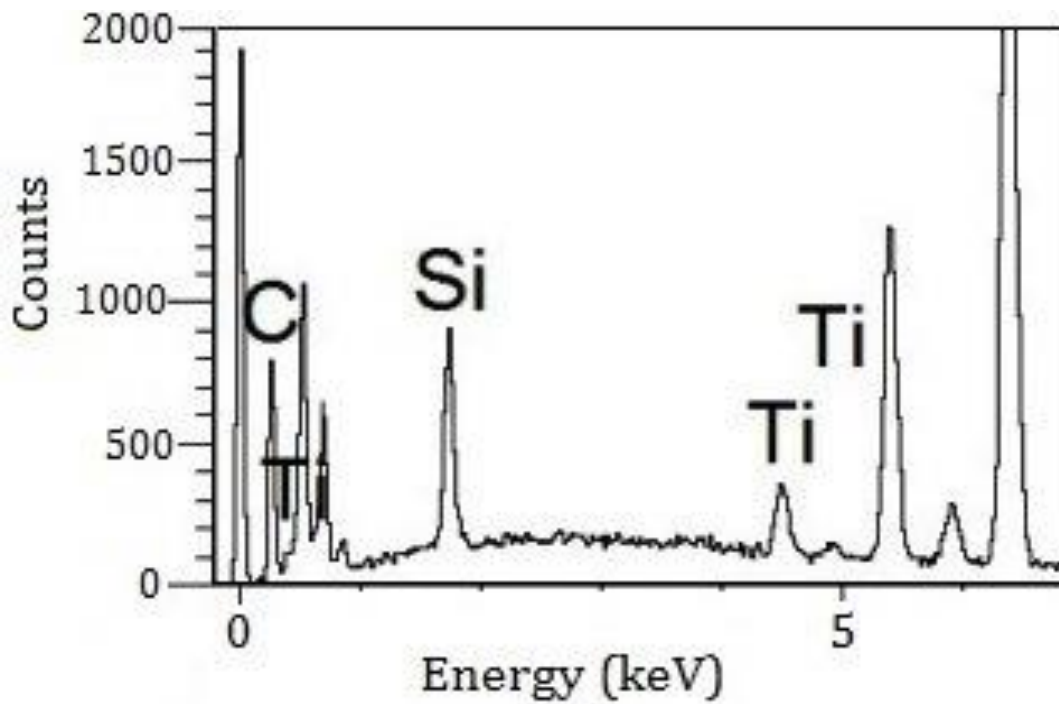


Fig. 3. EDX spectrum of the deposited steel substrate.

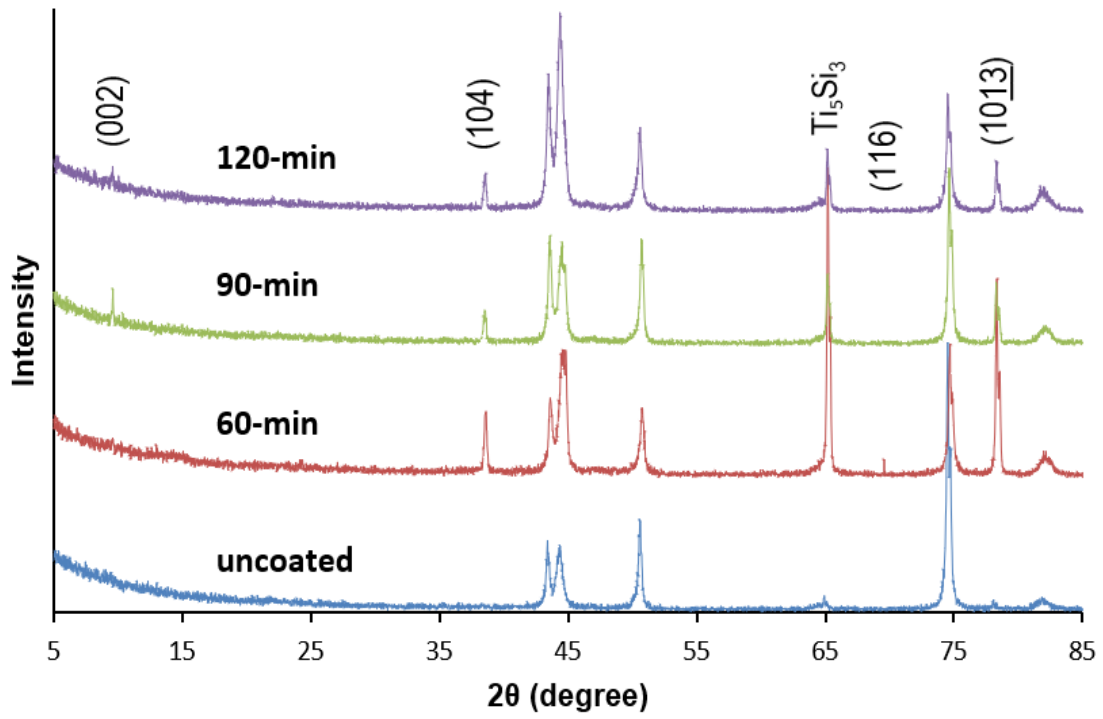


Fig. 4. XRD scans of the Ti₃SiC₂-coated steel substrates (Unlabeled peaks are inherent from the steel substrate).

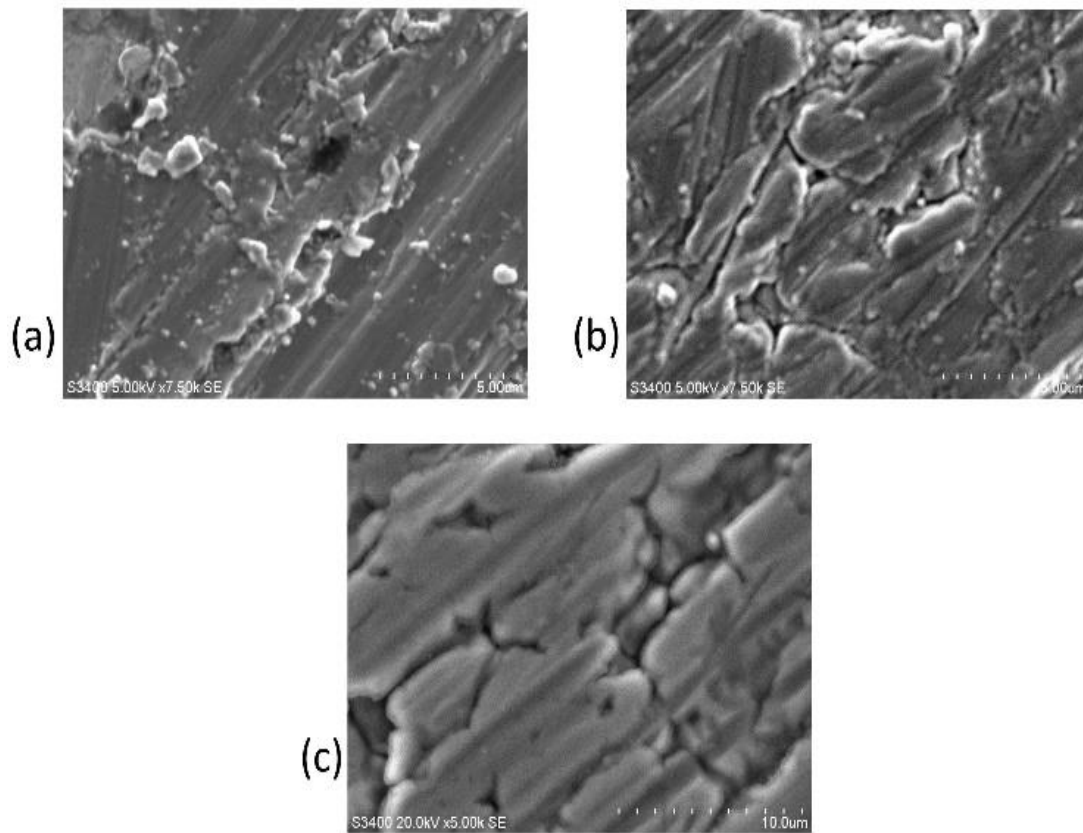


Fig. 5. SEM images of the samples synthesized at deposition times of (a) 60 min, (b) 90 min, and (c) 120 min.

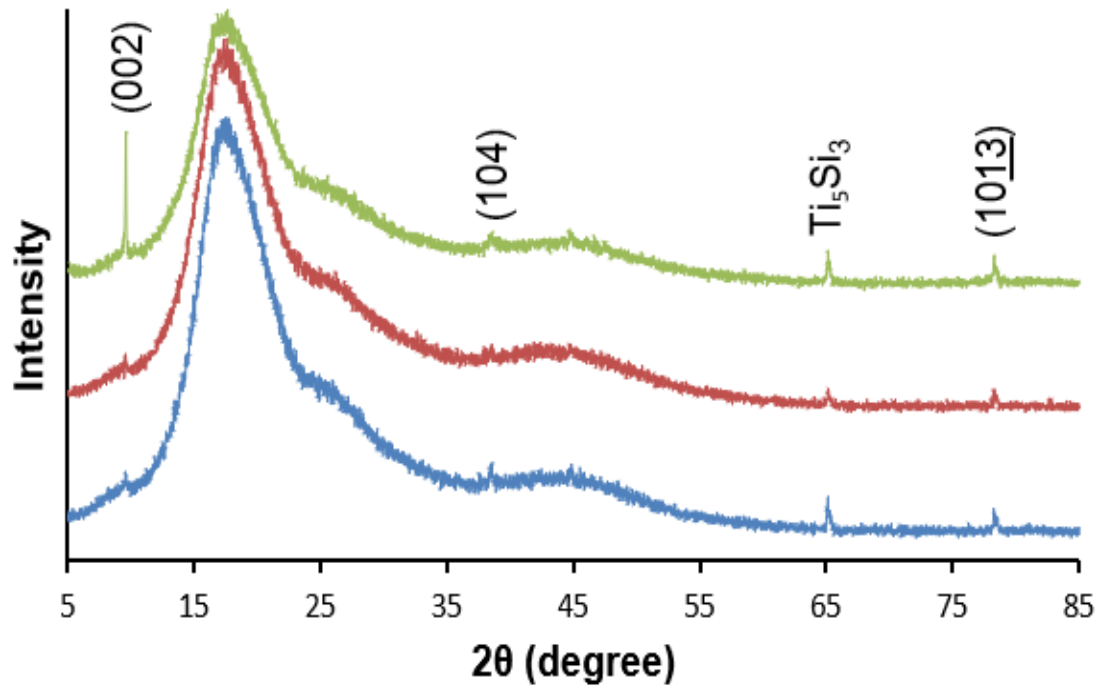


Fig. 6. XRD scans of the Ti_3SiC_2 -coated polycarbonate films.

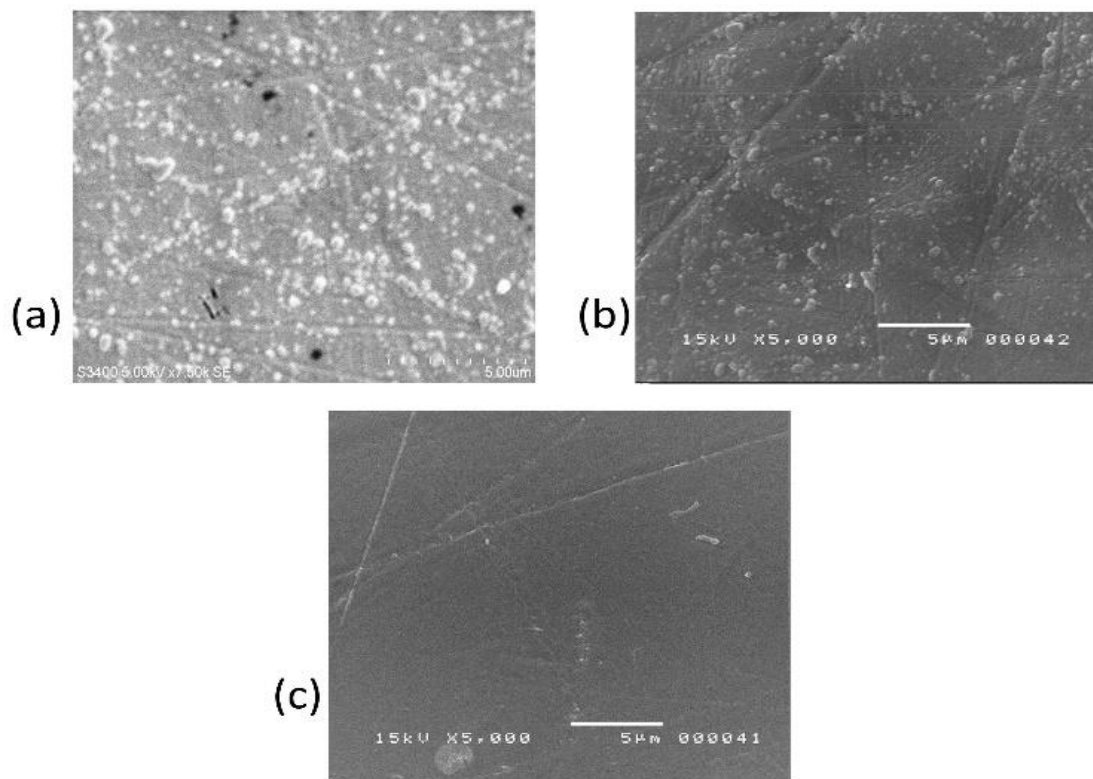


Fig. 7. SEM images of the polycarbonate film samples synthesized at deposition times of (a) 60 min, (b) 90 min, and (c) 120 min.

Table 1. FWHM and lattice properties of the samples synthesized at varying deposition time.

Sample's Deposition Time	2 θ (°)	Intensity (count/s)	FWHM (°)	D (nm)	ϵ (%)
60 min	78.32	640.23	0.168	61.0	0.09
90 min	78.29	200.35	0.168	61.0	0.09
120 min	78.31	163.27	0.120	85.4	0.064

4. Conclusions

The MAX phase compound Ti_3SiC_2 was effectively synthesized in thin film and deposited on stainless steel and polycarbonate substrates using a magnetized sheet plasma source without substrate heating and biasing. XRD results confirmed the successful synthesis of the ternary compound as the peaks corresponding to (002), (104), (116), and (1013) phases of Ti_3SiC_2 were observed. Based on the intensity of the XRD peaks, the content of Ti_3SiC_2 is greater when the deposition time was set at 60 min. Also, the surface of the coated steel substrate is smoother with grain formations as the deposition time was increased from 60 min to 120 min. For future studies, it would be beneficial to examine the physical, thermal, electrical, and other functional properties of the prepared Ti_3SiC_2 -coated steel and polycarbonate substrates for potential industrial applications.

Acknowledgment

The authors would like to thank the PCIEERD-DOST for the research grant under the Faculty Immersion Program.

References

- [1] M. W. Barsoum. (2000). The $Mn_{n+1}AX_n$ phases: A new class of solids: Thermodynamically stable nanolaminates. *Progress in solid state chemistry*. 28 (1-4): 201-281.
- [2] P. Eklund, M. Beckers, U. Jansson, H. Högberg, & L. Hultman. (2010). The $Mn_{n+1}AX_n$ phases: Materials science and thin-film processing. *Thin Solid Films*. 518 (8): 1851-1878.
- [3] Z. M. Sun. (2011). Progress in research and development on MAX phases: a family of layered ternary compounds. *International Materials Reviews*. 56 (3): 143-166.
- [4] C. Hu, H. Zhang, F. Li, Q. Huang, & Y. Bao. (2013). New phases' discovery in MAX family. *International Journal of Refractory Metals and Hard Materials*. 36: 300-312.
- [5] M. W. Barsoum, H. I. Yoo, I. K. Polushina, V. Y. Rud, Y. V. Rud, & T. El-Raghy. (2000). Electrical conductivity, thermopower, and hall effect of Ti_3AlC_2 , Ti_4AlN_3 , and Ti_3SiC_2 . *Physical Review B*. 62 (15): 10194.
- [6] N. F. Gao, Y. Miyamoto, & D. Zhang. (1999). Dense Ti_3SiC_2 prepared by reactive HIP. *Journal of materials science*. 34: 4385-4392.
- [7] Z. Sun, Z. Zhang, H. Hashimoto, & T. Abe. (2002). Ternary compound Ti_3SiC_2 : part I. Pulse discharge sintering synthesis. *Materials Transactions*. 43 (3): 428-431.
- [8] M. Sokol, V. Natu, S. Kota, & M. W. Barsoum. (2019). On the chemical diversity of the MAX phases. *Trends in Chemistry*. 1 (2): 210-223.
- [9] H. Aghamohammadi, A. Heidarpour, & R. Jamshidi. (2018). The phase and morphological evolution of Ti_3SiC_2 MAX phase powder after HF treatment. *Ceramics International*. 44 (15): 17992-18000.
- [10] K. Chen, X. Bai, X. Mu, P. Yan, N. Qiu, Y. Li, ... & Q. Huang. (2021). MAX phase Zr_2SeC and its thermal conduction behavior. *Journal of the European Ceramic Society*. 41 (8): 4447-4451.
- [11] S. Gupta, & M. W. Barsoum. (2011). On the tribology of the MAX phases and their composites during dry sliding: A review. *Wear*. 271 (9-10): 1878-1894.
- [12] J. G. Gigax, M. Kennas, H. Kim, T. Wang, B. R. Maier, H. Yeom, ... & L. Shao. (2019). Radiation response of Ti_2AlC MAX phase coated Zircaloy-4 for accident tolerant fuel cladding. *Journal of Nuclear Materials*. 523: 26-32.
- [13] C. Furgeaud, F. Brenet, & J. Nicolai. (2019). Multi-scale study of Ti_3SiC_2 thin film growth mechanisms obtained by magnetron sputtering. *Materialia*. 7: 100369.
- [14] H. Fashandi, M. Dahlqvist, J. Lu, J. Palisaitis, S. I. Simak, I. A. Abrikosov, ... Eklund. (2017). Synthesis of Ti_3AuC_2 , $Ti_3Au_2C_2$ and Ti_3IrC_2 by noble metal substitution reaction in Ti_3SiC_2 for high-temperature-stable Ohmic contacts to SiC. *Nature materials*. 16 (8): 814-818.
- [15] S. N. Perevislov, T. V. Sokolova, & V. L. Stolyarova. (2021). The Ti_3SiC_2 max phases as promising materials for high temperature applications: Formation under various synthesis conditions. *Materials Chemistry and Physics*. 267: 124625.

- [16] E. Tabares, A. Jiménez-Morales, & S. A. Tsipas. (2021). Study of the synthesis of MAX phase Ti₃SiC₂ powders by pressureless sintering. *Boletín de la Sociedad Española de Cerámica y Vidrio*. 60 (1): 41-52.
- [17] S. B. Li, J. X. Xie, L. T. Zhang, & L. F. Cheng. (2005). Synthesis and some properties of Ti₃SiC₂ by hot pressing of Ti, Si and C powders Part 2– Mechanical and other properties of Ti₃SiC₂. *Materials science and technology*. 21 (9): 1054-1058.
- [18] K. Tang, C. A. Wang, X. Xu, & Y. Huang. (2002). A study on powder X-ray diffraction of Ti₃SiC₂. *Materials Letters*. 55 (1-2): 50-54.
- [19] H. M. D. Barra, & H. J. Ramos. (2011). Deposition Rate and Energy Enhancements of TiN Thin-Film in a Magnetized Sheet Plasma Source. *International Journal of Materials and Metallurgical Engineering*. 5 (2): 114-116.
- [20] V. R. Noguera, & H. J. Ramos. (2006). A magnetized sheet plasma source for the synthesis of TiN on stainless steel substrates. *Thin Solid Films*. 506: 613-616.